Generalized model for photo-induced surface structure in amorphous thin films

Chao Lu, Daniel Recht, and Craig Arnold*
Princeton University
(Dated: January 24, 2013)

We present a generalized model to explain the spatial and temporal evolution of photoinduced surface structure in photosensitive amorphous thin films. The model is constructed by employing an incompressible viscous fluid model, driven by a photoinduced pressure originating from dipole rearrangement. In the derivation, one only requires the polarizability, viscosity and surface tension of the system. We check validity of the model by fitting to experimental data of As_2S_3 and demonstrating good agreement using two free fitting parameters.

INTRODUCTION

It has long been known that photoinduced surface relief structures are generated on a variety of materials like azobenzene-containing polymers, chalcogenides (like As_2S_3, AsSe, GeAsSe) and other amorphous materials [1–4]. Macroscopic surface structures can be inscribed by having periodic variations in intensity or polarization of the laser field [5]. This phenomenon is potentially useful for technologies such as rewritable optical data storage, active optical devices, nanofabrication, and optical actuators [6, 7]. However, a complete description of the underlying microscopic mechanism remains lacking.

In the past decades, much experimental and theoretical work has been performed to clarify the mechanism of this phenomenon. A number of models have been proposed to describe the formation process [2, 8], where volumetric internal pressure, interaction among dipoles, anisotropic diffusion or optical gradient forces have been considered as the driving force for surface restructurings [9–11]. In spite of the efforts, a unified model to capture all experimental observations remains lacking.

In this paper, we develop a two-stage model, wherein we first consider the generation of photoinduced pressure as a driving mechanism that initiates mass transport of the film, and in the second step we study the flow of material resulting from the application of this internal force. The flow of material is described using the Navier-Stokes equations for viscous flow. In the model, one assumes that the optical-induced pressure, is large enough to provide a driving force for mass transport, dependent on the intensity and polarization of the light. Finally we compare the model to the specific case of As_2S_3, simulation shows the surface height evolution as a function of time agrees with experimental measurements well.

THE MODEL

Fluid Dynamics of Surface Relief Formation

We assume that in the presence of optical radiation, the weak connections between the functional units in the chalcogenide glass, i.e. the van der waals forces, is broken, allowing these units to rearrange. Further stipulating laminar flow of the glass and time-independent illumination that varies in one direction along the surface (the x axis) but is uniform along the other surface axis (y) and with depth (z) brings surface relief formation in the thin films within the scope of the Navier-Stokes equation simplified into a two-dimensional boundary layer equation in x and z [12] (see figure 1).

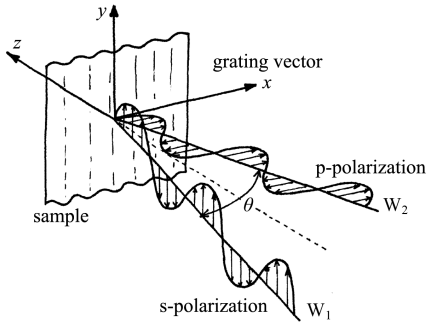

FIG. 1. Schematic diagram of the typical experimental setup used to generate surface structure.Two beams, W1 and W2, interfere on the surface of a thin film of amorphous light-sensitive material, leading to the pictured definitions of the coordinate system and polarization directions.

$$\frac{\partial v_x}{\partial t} + v_x\frac{\partial v_x}{\partial x} + v_z\frac{\partial v_x}{\partial z} = -\frac{1}{\rho}\frac{\partial \mathcal{P}}{\partial x} + \nu\frac{\partial^2 v_x}{\partial z^2} + f, \quad (1)$$

in which the v_i's are components of the velocity vector, ρ is the mass density, $\mathcal{P}$ is the total pressure, f is the body force, and ν is the kinematic viscosity. Applying a thin-film approximation sanctions the replacement of $\mathcal{P}$ with its value at the surface since there is little depth over which the pressure can change. At the surface, $\mathcal{P}$ is comprised of surface tension, $\mathcal{S}$, and the photoinduced pressure, P. Surface tension is traditionally taken to be proportional to surface curvature. Symbolically

$$\mathcal{S} = \sigma\frac{\frac{d^2h}{dx^2}}{\left[1+\left(\frac{dh}{dx}\right)^2\right]^{3/2}} \approx \sigma\frac{d^2h}{dx^2}, \quad (2)$$

where h is the (spatially varying) thickness of the film, and the last step is justified by the thin film approximation since this condition implies $dh/dx \ll 1$. The photoinduced pressure, which is simply assumed to exist, is discussed at length in the following section. For now it is enough to note that since the illumination is modulated only along the x axis, the photoinduced pressure can vary only with x. The thin film approximation thus makes it possible to write

$$\mathcal{P} \approx P(x) - \sigma \frac{\partial^2 h}{\partial x^2}. \tag{3}$$

In addition, we assume there are no body forces so $f = 0$.

Combining this information with equation 1 leads to

$$\frac{\partial v_x}{\partial t} + v_x \frac{\partial v_x}{\partial x} + v_z \frac{\partial v_x}{\partial z} = -\frac{1}{\rho}\frac{\partial}{\partial x}\left[P(x) - \sigma \frac{\partial^2 h}{\partial x^2}\right] + \nu \frac{\partial^2 v_x}{\partial z^2}. \tag{4}$$

The thin film approximation also implies that

$$v_x \frac{\partial v_x}{\partial x} \ll v_z \frac{\partial v_x}{\partial z} \tag{5}$$

since v_x and v_z are of roughly the same order and the film is assumed to be much wider than it is thick. Following the analyses of Ledoyen et al. and Pimputkar et al., it is possible to drop all the terms on the right-hand side because they turn out to be small in practice [13–15]. Doing so yields

$$\frac{\partial^2 v_x}{\partial z^2} \approx \frac{1}{\eta}\left[\frac{\partial P(x)}{\partial x} - \sigma \frac{\partial^3 h}{\partial x^3}\right], \tag{6}$$

where $\eta = \rho\nu$ is the dynamic viscosity.

Equation 6 is solvable subject to the following constraints and boundary conditions. First, we have the continuity equation

$$\frac{\partial v_x}{\partial x} + \frac{\partial v_z}{\partial z} = 0, \tag{7}$$

which is derived from incompressibility and conservation of mass. Next, assuming perfect adhesion to the substrate implies

$$v_x = v_z = 0 \text{ at } z = 0, \tag{8}$$

where $z = 0$ is the film-substrate interface. At the free surface of the film, the shear stress along z goes to zero [12, 15]. Symbolically,

$$\frac{\partial v_x}{\partial z} = 0 \text{ at } z = h. \tag{9}$$

Finally, the z velocity at the free surface is the rate of change in the height. This can be represented formally as

$$v_z = \frac{\partial h}{\partial t} \text{ at } z = h. \tag{10}$$

Since the right-hand side of equation 6 has no z dependence, the whole equation can be integrated with respect to z.

$$\frac{\partial v_x}{\partial z} \approx \frac{z}{\eta}\left[\frac{\partial P(x)}{\partial x} - \sigma \frac{\partial^3 h}{\partial x^3}\right] + C_1, \tag{11}$$

where C_1 is an integration constant. Applying the shear stress boundary condition (equation 9) yields C_1. Thus

$$\frac{\partial v_x}{\partial z} \approx \frac{(z-h)}{\eta}\left[\frac{\partial P(x)}{\partial x} - \sigma \frac{\partial^3 h}{\partial x^3}\right]. \tag{12}$$

Integrating with respect to z again gives

$$v_x \approx \frac{\left(z^2/2 - hz\right)}{\eta}\left[\frac{\partial P(x)}{\partial x} - \sigma \frac{\partial^3 h}{\partial x^3}\right] + C_2. \tag{13}$$

The application of equation 8 clearly shows that C_2 is 0. Taking the derivative of both sides with respect to x and applying the continuity condition of equation 7 yields

$$-\frac{\partial v_z}{\partial z} \approx \frac{\partial}{\partial x}\left(\frac{\left(z^2/2 - hz\right)}{\eta}\left[\frac{\partial P(x)}{\partial x} - \sigma \frac{\partial^3 h}{\partial x^3}\right]\right). \tag{14}$$

This too can be integrated with respect to z.

$$-v_z \approx \frac{\partial}{\partial x}\left(\frac{\left(z^3/6 - hz^2/2\right)}{\eta}\left[\frac{\partial P(x)}{\partial x} - \sigma \frac{\partial^3 h}{\partial x^3}\right]\right) + C_3 \tag{15}$$

Equation 8 once again reveals C_3 to be 0 as well.

Finally, setting $z = h$ and applying the last boundary condition of equation 10 gives

$$\frac{\partial h}{\partial t} \approx \frac{\partial}{\partial x}\left(\frac{h^3}{3\eta}\left[\frac{\partial P(x)}{\partial x} - \sigma \frac{\partial^3 h}{\partial x^3}\right]\right). \tag{16}$$

Now the optical induced pressure $P(x)$ is the only quantity that remains to be determined. Given a of $P(x)$, equation 16 is readily solvable by standard numerical methods.

The Optical-induced Pressure

We assert that the pressure arises from the electric field of the incident light. The diffusion units, which are size of medium order range (up to 2 coordination sphere), are simplified to be the electrical-induced dipoles. The strength of the dipoles can be calculated by the equation $\vec{P} = \int d^3 r \rho(\vec{r}) \vec{r}$, where the charge distribution $\rho(\vec{r})$ can be obtained from high accuracy first principle calculations. Those dipoles begin to align and move according to the polarization of the electrical field, until a new balance is achieved, where the secondary bonding is reconstructed. It is by this way, the units diffuse, leading to the surface morphology modified by the optical field.

We are able to calculate the photo-induced pressure. Since pressure is always proportional to energy density we start with relation $Pressure \propto \partial Energy/\partial V$. Equations describing the total free energy density of such dipole interaction system in the presence of an electric field are given by Landau [16],

$$Energy = F_0 + \epsilon_{ik}\epsilon_0 E_i E_k. \tag{17}$$

Where F_0 is the free energy of the system in absence of an external field. In the dipole interaction model, ϵ_{ik}, component of the relative permittivity tensor, describes the polarizability of diffusion units when exposed to electric field of the light. Rigorous results for the pressure are obtained from equation 17, in terms of the stress tensor.

$$\sigma_{ik} = \epsilon_0 E_i D_k. \tag{18}$$

Plugging $D_k = \Sigma(\epsilon_{km} E_m)$ into equation 18, the stress tensor is simplified as

$$\sigma_{ik} = \epsilon_0 E_i(\epsilon_{kx}E_x + \epsilon_{ky}E_y + \epsilon_{kz}E_z). \tag{19}$$

Now we assume that the electric field oscillates so quickly that one could not reasonably expect the material to respond to it in other than a time-averaged manner. Thus taking the trace of the stress tensor and calculating the time average, we can write the pressure as

$$\begin{aligned} P &= \frac{1}{3}\langle Trace(\sigma)\rangle \\ &= \frac{1}{3}\langle \sigma_{xx} + \sigma_{yy} + \sigma_{zz}\rangle \\ &= \frac{\epsilon_0}{3}\langle E_x(\epsilon_{xx}E_x + \epsilon_{xy}E_y) + E_y(\epsilon_{yx}E_x + \epsilon_{yy}E_y)\rangle \\ &= \frac{\epsilon_0}{3}\langle \epsilon_{xx}E_x^2 + 2\epsilon_{xy}E_xE_y + \epsilon_{yy}E_y^2\rangle . \end{aligned} \tag{20}$$

Absent from equation 20 is a provision to ensure that the pressure is real. Two choices can be thrown away immediately: taking the real part of the entire right-hand side of equation 20 and saying that $P(E_x, E_y) = P(|E_x|, |E_y|)$. The former leads to pressures that oscillate rapidly in time about a mean of 0. The latter ignores all phase information and thus cannot hope to explain s-p interference.

The appropriate choice is to require that $P(E_x, E_y) = P(\tilde{E_x}, \tilde{E_y})$ where $\tilde{E_x} = \Re\mathrm{e}\{E_x\}$. In this case, equation 20 becomes

$$\begin{aligned} P(E_x, E_y) &= P(\tilde{E_x}, \tilde{E_y}) \\ &= \frac{\epsilon_0}{3}\langle \epsilon_{xx}\tilde{E_x}^2 + 2\epsilon_{xy}\tilde{E_x}\tilde{E_y} + \epsilon_{yy}\tilde{E_y}^2\rangle . \end{aligned} \tag{21}$$

The coefficients in equation 21, which describe the polarizablity of the material, could be measured experimentally. With these coefficients, the pressure is readily calculated.

Equation 21 together with 16, completes our model explaining optical induced surface roughing phenomenon. All the coefficients are determined by the properties of the material: η, the dynamic viscosity, describes the mobility; σ is a constant related to the surface tension; while ϵ_{ik} reflect the photo sensitivity to the external fields. In reality, some materials may have lower mobility, or are less sensitive to the light, making the pressure driven term small, such that the surface structure formation is annihilated by the surface tension. This suggests the model to be an generalized one, as long as the required conditions are satisfied, i.e., the material is amorphous and thin in z direction.

SIMULATION

To check the validity of the model, we calculate the solution to equation 16 on a typical holographic setup used to generate surface structure (see FIG.1). In the setups, everything about the two interfering beams is identical except for the direction of their wave vectors and possibly their polarization. The most generic electric field produced by such interference can then be written

$$e^{i(kx-\omega t)}\begin{pmatrix} |E_x|\, e^{i\phi_x} \\ |E_y|\, e^{i\phi_y} \end{pmatrix}, \tag{22}$$

where $|E_x|$, $|E_y|$, ϕ_x, and ϕ_y are arbitrary, real, and time (but not necessarily position) independent. Taking E_x and E_y from 22, plugging them into 21, and computing the time averages gives

$$P = b_1 |E_x|^2 + b_2 |E_y|^2 + b_3 |E_x|\,|E_y| \cos\Delta\phi, \tag{23}$$

where $b_1 = \epsilon_0\epsilon_{xx}/6$, $b_2 = \epsilon_0\epsilon_{yy}/6$ and $b_3 = \epsilon_0\epsilon_{xy}/3$. Defining a generalized polarization angle (applicable to elliptical polarizations) $\psi = \arctan|E_y|/|E_x|$, equation 23 can be rewritten as

$$P = I\left[b_1\cos^2\psi + b_2\sin^2\psi + b_3\sin 2\psi\cos\Delta\phi\right] \tag{24}$$

$$= I(x)\left[c_1 + c_2\cos 2\psi(x) + c_3\cos\Delta\phi(x)\sin 2\psi(x)\right], \tag{25}$$

where the x dependence explicitly indicated in going from equation 24 to equation 25, while the coefficients have been redefined and calculated as: $c_1 = \epsilon_0\epsilon_{xx}/6$, $c_2 = \epsilon_0(\epsilon_{yy} - \epsilon_{xx})/6$ and $c_3 = \epsilon_0\epsilon_{xy}/3$. Equation 25 is intuitively reasonable since it depends on intensity, polarization, and $\Delta\phi$, the three quantities whose modulation have been experimentally shown to cause surface relief

Polarization	$I(x)$	$\psi(x)$	$\Delta\phi(x)$	$P(x)$
s-s	$2E_0^2\,(1+\cos 2\delta)$	$\pi/2$	0	$(c_1-c_2)2E_0^2\,(1+\cos 2\delta)$
p-p	$2E_0^2\,(1+\cos 2\delta)$	0	0	$(c_1+c_2)2E_0^2\,(1+\cos 2\delta)$
s-p	$2E_0^2$	$\pi/4$	-2δ	$2E_0^2\,(c_1+c_3\cos 2\delta)$
45-135	$2E_0^2$	δ	$-\pi/2$	$2E_0^2\,(c_1+c_2\cos 2\delta)$
LCP-RCP	$2E_0^2$	δ	0	$2E_0^2\,(c_1+c_2\cos 2\delta+c_3\sin 2\delta)$
				$=2E_0^2\left(c_1+\sqrt{c_2^2+c_3^2}\sin\left[2\delta+\arctan\left(c_3/c_2\right)\right]\right)$

TABLE I. Summary of the photoinduced pressure predicted by equation 25 for various polarization conditions. I, ψ, and $\Delta\phi$ can easily be derived from the interference of plane waves. $\delta=\frac{2\pi}{\lambda}x\sin\frac{\theta}{2}$ for θ as in figure 1. A trigonometric identity was used to derive the second form of $P(x)$ for LCP-RCP interference in order to show that for all cases considered $P(x)$ can be expressed as twice the intensity of one of the initial beams times the sum of a constant and a sinusoidal oscillation.

[2, 17]. Taking the first spatial derivative of Equation 25 yields

$$\begin{aligned}\frac{\partial P}{\partial x}=&\frac{\partial I}{\partial x}\left[c_1+c_2\cos 2\psi(x)+c_3\cos\Delta\phi(x)\sin 2\psi(x)\right]\\&+2I(x)\frac{\partial\psi}{\partial x}\left[-c_2\sin 2\psi(x)+c_3\cos\Delta\phi(x)\cos 2\psi(x)\right]\\&+I(x)\frac{\partial\Delta\phi}{\partial x}\left[-c_3\sin\Delta\phi(x)\sin 2\psi(x)\right].\end{aligned}\tag{26}$$

Equation 26 cleanly separates into three independent terms governing the pressure gradient induced by modulation of intensity, polarization direction, and phase. Accordingly, this model is consistent with the idea suggested by the data that the intensity and phase modulation terms arise from the scalar effect while the angle modulation term is due to the vector phenomenon.

Table I lists the pressure functions predicted by equation 25 for the common used polarization conditions. Despite the widely varying initial conditions considered, the $P(x)$'s can all be represented by the same general form. Recalling typically E_0^2 has a Gaussian profile, we reexpress the pressure as

$$P(x)=p_1e^{-2(x/p_2)^2}\left[p_3+\cos\left(p_4x+p_5\right)\right]\tag{27}$$

where the p_i's are, parameters decided either by the experimental setup or the properties of the material. p_2 is fixed as the modulation frequency, and p_4 is the beam radius, which are the same across all polarization conditions; with p_5 included to account for the possibility that the Gaussian intensity profile is not centered on a peak of the modulation. On the other hand, p_1 and p_3, are parameters of the material, whose value are measured by fitting the model with the experimental data.

Figure 2 demonstrates the dynamics of light induced grating construction of arbitrary materials, each of which is denoted by a set of parameters $\{p_1,\ \sigma,\ \eta\}$. Grating amplitudes increase as a function of time, due to the accumulation of irradiation. However, under the regime of very high surface tension or viscosity, we see no increase in the amplitude corresponding to the case where the optical-induced forces are not sufficient to overcome the energy barrier, as shown in line A. In the figure, curve A and C have the same viscosity, but the surface tension in C is lower, so the grating heights grow much faster. While the surface tension of B and C are the same, the growth rate in C is higher because of its smaller viscosity. Comparisons reveal that decreasing either η (viscosity) or σ (surface tension) promotes the formation of a grating, which agrees with the underlying physics.

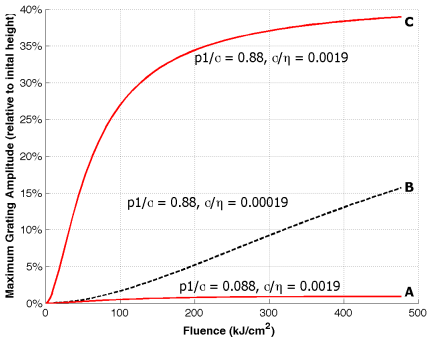

FIG. 2. Plots of maximum grating amplitude evolution versus irradiation fluence (time). Each curve coresponds to a set of material parameters: $\{p_1,\ \sigma,\ \eta\}$. Particularly, the upper curve, generated by $\{p1/\sigma=0.88\mu m^{-1},\ \sigma/\eta=0.0019\mu m/s\}$, simulates the response of As_2S_3.

RESULTS

In order to test our model against a real system, we compare it to an experimental result on As_2S_3[2]. Setting $c_2=3c_1$ and $c_3=2c_1$ begins to approximate Saliminia's qualitative description of the observed size ordering. This not only implies the well-known anisotropy response of As_2S_3, when exposed to external optical field, but also reveals the quantitative relationship: $\epsilon_{yy}=4\epsilon_{xx}$, $\epsilon_{xy}=\epsilon_{xx}$.

The model parameters are summarized in table II. Simulation results demonstrate the consistency between the model and experiments. Figure 3 shows the model's

Parameter	Meaning	Value
	Fixed Parameters	
h_0	Initial Thickness	2 μm
T	Total Illumination Time	381 s
p_2	Illumination Radius	57 μm
p_3	Non-Oscillatory Pressure	1
p_4	Modulation Frequency	$2\pi/13$ μm^{-1}
p_5	Modulation Phase	$\pi/2$
	Free Parameters	
p_1/σ	Relative Pressure Strength	0.88 μm^{-1}
σ/η	Characteristic Growth Rate	1.9×10^{-3} μm/s

TABLE II. Summary of the parameters used in constructing the fit depicted in figure 3.

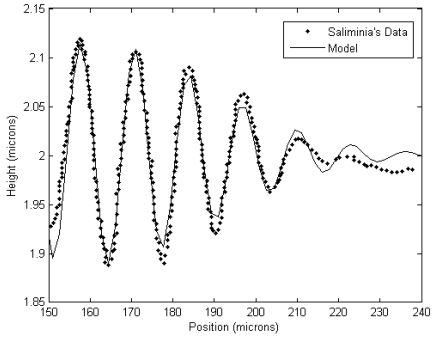

FIG. 3. The model's fit to a section of a surface relief profile data from [2]. Results generated by model agrees well with experimental measurements, both in amplitude and frequency.

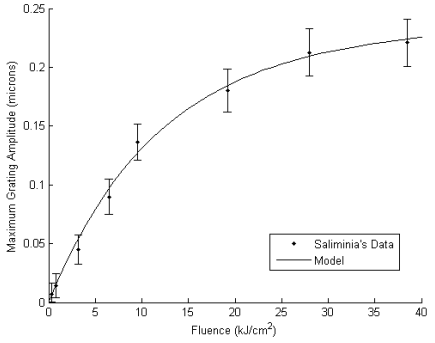

FIG. 4. Fluence (time) dependence of maximum surface relief amplitude for the fit in figure 3.

fit to a section of a surface relief profile from [2]. This fit matches both the frequency and amplitude over large space given by realistic experimental parameters. In order to further verify the quality of this model, we compare the time dependence of the maximum surface relief amplitude as shown in figure 4. The grating amplitude, as a function of time, is increasing with a decreasing rate, until it eventually saturates at higher fluence. Once again we see that within experimental uncertainty we have a good fit to the data, indicating this approach is reasonable.

In summary, the goal of this work was to study the mechanism of mass transport, which results in surface morphology changes, when external stimuli are applied to chalcogenide materials, especially As_2S_3. We applied the Navier-Stokes equation to describe the dynamics of surface structure change, together with a dipole interaction model to calculate the driving force – the optical-induced pressure. With the derived equation of motion, simulation results are obtained, which agree with the experimental data well, demonstrating the validity of the model, when applied to chalcogenide materials.

This work was supported by National Science Foundation (NSF) grant EEC-0540832.

* cbarnold@princeton.edu

[1] N. K. Viswanathan, S. Balasubramanian, L. Li, J. Kumar, and S. K. Tripathy, The Journal of Physical Chemistry B **102**, 6064 (1998).

[2] A. Saliminia, T. V. Galstian, and A. Villeneuve, Physical Review Letters **85**, 4112 (2000).

[3] S. SHTUTINA, M. KLEBANOV, V. LYUBIN, S. ROSENWAKS, and V. VOLTERRA, Thin Solid Films **261**, 263 (1995).

[4] D. Barada, M. Itoh, and T. Yatagai, Journal of Applied Physics **96**, 4204 (2004).

[5] X. L. Jiang, L. Li, J. Kumar, D. Y. Kim, and S. K. Tripathy, Applied Physics Letters **72**, 2502 (1998).

[6] K. Harada, H. Inoue, M. A. El-Morsy, M. Itoh, S. Umegaki, and T. Yatagai, Japanese Journal of Applied Physics **41**, 1851 (2002).

[7] D. Y. Kim, S. K. Tripathy, L. Li, and J. Kumar, Applied Physics Letters **66**, 1166 (1995).

[8] H. Hisakuni and K. Tanaka, Science **270**, 974 (1995).

[9] J. Kumar, L. Li, X. L. Jiang, D.-Y. Kim, T. S. Lee, and S. Tripathy, Applied Physics Letters **72**, 2096 (1998).

[10] S. Bian, J. M. Williams, D.-Y. Kim, L. Li, S. Balasubramanian, J. Kumar, and S. Tripathy, Journal of Applied Physics **86**, 4498 (1999).

[11] P. Lefin, C. Fiorini, and J.-M. Nunzi, Pure and Applied Optics: Journal of the European Optical Society Part A **7**, 71 (1999).

[12] V. Levich, *Physiochemical Hydrodynamics*, 2nd ed. (Prentice-Hall, Englewood Cliffs, NJ, 1962) pp. 372-376 and 669-671.

[13] F. Ledoyen, P. Bouchard, D. Hennequin, and M. Cormier, Physical Review A **41**, 4895 (1990).

[14] S. Pimputkar and S. Ostrach, Physics of Fluids **23**, 1281 (1980).

[15] C. J. Barrett, P. L. Rochon, and A. L. Natansohn, Journal of Chemical Physics **109**, 1505 (1998).

[16] L. D. Landau and E. M. Lifshitz, *Electrodynamics of Continuous Media* (Pergamon Press LTD., 1960) pp. 58-69.

[17] K. Tanaka, Journal of Optoelectronics and Advanced Materials **7**, 2571 (2005).